1. Introduction

The first indication of the quantum nature of light came in 1900 when M. Planck discovered he could account for the spectral distribution of thermal light by postulating that the energy of a harmonic oscillator is quantized. Further evidence was added by A. Einstein who showed in 1905 that the photoelectric effect could be explained by the hypothesis that the energy of a light beam was distributed in discrete bundles later known as photons.

Einstein also contributed to the understanding of the absorption and emission of light from atoms with his development of a phenomenological theory in 1917. This theory was later shown to be a natural consequence of the quantum theory of electromagnetic radiation.

Despite this early connection with quantum theory physical optics has developed more or less independently of quantum theory. The vast majority of physical-optics experiments can adequately be explained using classical theory of electromagnetic radiation based on Maxwell's equations. An early attempt to find quantum effects in an optical interference experiment by G.I. Taylor in 1909 gave a negative result. Taylor's experiment was an attempt to repeat T. Young's famous two slit experiment with one photon incident on the slits. The classical explanation based on the interference of electric field amplitudes and the quantum explanation based on the interference of the probability amplitudes for the photon to pass through either slit coincide in this experiment. Interference experiments of Young's type do not distinguish between the predictions of classical theory and quantum theory. It is only in higher-order interference experiments involving the interference of intensities that differences between the predictions of classical and quantum theory appear. In such an experiment two electric fields are detected on a photomultiplier and their intensities are allowed to interfere. Whereas classical theory treats the interference of intensities, in quantum theory the interference is still at the level of probability amplitudes. This is one of the most important differences between quantum theory and classical theory.

The first experiment in intensity interferometry was the famous experiment of R. Hanbury Brown and R.Q. Twiss. This experiment studied the correlation in the photo-current fluctuations from two detectors. Later experiments were photon counting experiments, and the correlations between photon numbers were studied.

The Hanbury–Brown–Twiss experiment observed an enhancement in the two-time intensity correlation function of short time delays for a thermal light source known as photon bunching. This was a consequence of the large intensity fluctuations in the thermal source. Such photon bunching phenomena may be adequately explained using a classical theory with a fluctuating electric field amplitude. For a perfectly amplitude stabilized light field such as an ideal laser operating well above threshold there is no photon bunching. A photon counting experiment where the number of photons arriving in an interval T are counted, shows that there is still a randomness in the photon arrivals. The photon-number distribution for an ideal laser is Poissonian. For thermal light a super-Poissonian photocount distribution results.

While the above results may be derived from both classical and quantum theory, the quantum theory makes additional unique predictions. This was first elucidated by R.J. Glauber in his quantum formulation of optical coherence theory in 1963. One such prediction is photon antibunching where the initial slope of the two-time correlation function is positive. This corresponds to greater than average separations between the photon arrivals or photon antibunching. The photocount statistics may also be sub-Poissonian. A classical theory of fluctuating field amplitudes would require negative probabilities in order to give photon antibunching. In the quantum picture it is easy to visualize photon arrivals more regular than Poissonian.

It was not, however, until 1975 when H.J. Carmichael and D.F. Walls predicted that light generated in resonance fluorescence from a two-level atom would exhibit photon antibunching that a physically accessible system exhibiting nonclassical behaviour was identified. Photon antibunching was observed during the next year in this system in an experiment by H.J. Kimble, M. Dagenais and L. Mandel. This was the first nonclassical effect observed in optics and ushered in a new era in quantum optics.

The experiments of Kimble et al. used an atomic beam and hence the photon antibunching was convolved with the atomic number fluctuations in the beam. With developments in ion-trap technology it is now possible to trap a single ion for several minutes. H. Walther and coworkers in Munich have studied resonance fluorescence from a single atom in a trap. They have observed both photon antibunching and sub-Poissonian statistics in this system.

In the 1960's improvements in photon counting techniques proceeded in tandem with the development of new laser light sources. Light from incoherent (thermal) and coherent (laser) sources could now be distinguished by their photon counting properties. The groups of F.T. Arecchi in Milan, L. Mandel in Rochester and R.E. Pike in Malvern measured the photocount statistics of the laser. They showed that the photocount statistics went from super-Poissonian below threshold to Poissonian far above threshold. Concurrently, the quantum theory of the laser was being developed by H. Haken in Stuttgart, M.O. Scully and W. Lamb at Yale, and M. Lax and W.H. Louisell in New Jersey. In these theories both the atomic variables and the electromagnetic field were quantized. The result of these calculations were that the laser functioned as an essentially classical device. In fact H. Risken showed that it could be modelled by a van der Pol oscillator.

It is only quite recently that the role the noise in the pumping process plays in obscuring the quantum aspects of the laser has been understood. If the noise in the pumping process can be suppressed the output of the laser may exhibit sub-Poissonian statistics. In other words, the intensity fluctuations may be reduced below the shot-noise level characteristic of normal lasers. Y. Yamamoto in Tokyo has pioneered experimental developments in the area of semiconductor lasers with suppressed pump noise. In a high impedance constant current driven semiconductor laser the fluctuations in the pumping electrons are reduced below Poissonian. This results in the photon statistics of the emitted photons being sub-Poissonian.

It took another nine years after the observation of photon antibunching for another prediction of the quantum theory of light to be observed – squeezing of quantum fluctuations. The electric field for a nearly monochromatic plane wave may be decomposed into two quadrature components with the time dependence $\cos \omega t$ and $\sin \omega t$, respectively. In a coherent state, the closest quantum counterpart to a classical field, the fluctuations in the two quadratures are equal and minimize the uncertainty product given by Heisenberg's uncertainty relation. The quantum fluctuations in a coherent state are equal to the zero-point vacuum fluctuations and are randomly distributed in phase. In a squeezed state the quantum fluctuations are no longer independent of phase. One quadrature phase may have reduced quantum fluctuations at the expense of increased quantum fluctuations in the other quadrature phase such that the product of the fluctuations still obeys Heisenberg's uncertainty relation.

Squeezed states offer the possibility of beating the quantum limit in optical measurements by making phase-sensitive measurements which utilize only the quadrature with reduced quantum fluctuations. The generation of squeezed states requires a nonlinear phase-dependent interaction. The first observation of squeezed states was achieved by R.E. Slusher in 1985 at the AT&T Bell Laboratories in four-wave mixing in atomic sodium. This was soon followed by demonstrations of squeezing in an optical parametric oscillator by H.J. Kimble and by four-wave mixing in optical fibres by M.D. Levenson.

Squeezing-like photon antibunching is a consequence of the quantization of the light field. The usefulness of squeezed light was demonstrated in experiments in optical interferometry by Kimble and Slusher. Following the original suggestion of C.M. Caves at Caltech they injected squeezed light into the empty port of an interferometer. By choosing the phase of the squeezed light so that the quantum fluctuations entering the empty port were reduced below the vacuum level they observed an enhanced visibility of the interference fringes.

In the nonlinear process of parametric down conversion a high frequency photon splits into two photons with frequencies such that their sum equals that of the high-energy photon. The two photons (photon twins) produced in this process possess quantum correlations and have identical intensity fluctuations. This may be exploited in experiments where the intensity fluctuations in the difference photocurrent for the two beams is measured. The intensity difference fluctuations in the twin beams have been shown to be considerably below the shot-noise level in experiments by E. Giacobino in Paris and P. Kumar in Evanston.

The twin beams may also be used in absorption measurements where the sample is placed in one of the beams and the other beam is used as a reference. The driving laser is tuned so that the frequency of the twin beams matches the frequency at which the sample absorbs. When the twin beams are detected and the photocurrents are subtracted, the presence of even very weak absorption can be seen because of the small quantum noise in the difference current.

The photon pairs generated in parametric down conversion also carry quantum correlations of the Einstein–Podolsky–Rosen type. Intensity correlation experiments to test Bell inequalities were designed using a correlated pair of photons. The initial experiments by A. Aspect in Paris utilized a two photon cascade to generate the correlated photons, however, recent experiments have used parametric down conversion. These experiments have consistently given results in agreement with the predictions of quantum theory and in violation of classical predictions. At the basis of the difference between the two theories is the interference of probability amplitudes which is characteristic of quantum mechanics. In these intensity interference experiments as opposed to interference experiments of the Young's type the two theories yield different predictions. This was strikingly demonstrated in an intensity interference experiment which has only one incident photon but has phase-sensitive detection. In this experiment proposed by S.M. Tan, D.F. Walls and M.J. Collett a single photon may take either path to two homodyne detectors. Nonlocal quantum correlations between the two detectors occur, which are a consequence of the interference of the probability amplitudes for the photon to take either path.

The major advances made in quantum optics, in particular the ability to generate and detect light with less quantum fluctuations than the vacuum, makes optics a fertile testing ground for quantum measurement theory. The idea of quantum non-demolition measurements arose in the context of how to detect the change in position of a free mass acted on by a force such as a gravitational wave. However, the concept is general. Basically one wishes to measure the value of an observable without disturbing it so that subsequent measurements can be made with equal accuracy as the first. Demonstrations of quantum non-demolition measurements have been achieved in optics. In experiments by M.D. Levenson and P. Grangier two electromagnetic-field modes have been coupled via a nonlinear interaction. A measurement of the amplitude quadrature of one mode (the probe) allows one to infer the value of the amplitude quadrature of the other mode (the signal) without disturbing it. This quantum non-demolition measurement allows one to evade the back action noise of the measurement by shunting the noise into the phase quadrature which is undetected.

The techniques developed in quantum optics include quantum treatments of dissipation. Dissipation has been shown to play a crucial role in the destruction of quantum coherence, which has profound implications for quantum measurement theory. The difficulties in generating a macroscopic superposition of quantum states (Schrödingers cat) is due to the fragility of such states to the presence of even small dissipation. Several schemes to generate these superposition states in optics have been proposed but to date there has been no experimental manifestation.

Matter-wave interferometry is a well established field, for example, electron and neutron interferometry. More recently, however, such effects have been demonstrated with atoms. Interferometry with atoms offers the advantage of greater mass and therefore greater sensitivity for measurements of changes of gravitational potentials. Using techniques of laser cooling the de Broglie wavelength of atoms may be increased. With slow atoms the passage time in the interferometer is increased thus leading to an increase in sensitivity. Atoms also have internal degrees of freedom which may be used to tag which path an atom took. Thus demonstrations of the principle of complementary using a double-slit interference experiment with which path detectors may be realized with atoms.

Atoms may be diffracted from the periodic potential structure of a standing light wave. A new field of atomic optics is rapidly emerging. In atomic optics the role of the light and atoms are reversed. Optical elements such as mirrors and beam splitters consist of light fields which reflect and split atomic beams. The transmission of an atom by a standing light wave may be state selective (the optical Stern–Gerlach effect) and this property may be used as a beam splitter. The scattering of an atom by a standing light wave may depend on the photon statistics of the light. Hence, measuring the final momentum distribution of the atoms may give information on the photon statistics of the light field. Thus atomic optics may extend the range of quantum measurements possible with quantum optical techniques. For example, the position an atom passes through a standing light wave may be determined by measuring the phase shift it imparts to the light.

The field of quantum optics now occupies a central position involving the interaction of atoms with the electromagnetic field. It covers a wide range of topics ranging from fundamental tests of quantum theory to the development of new laser-light sources. In this text we introduce the analytic techniques of quantum optics. These techniques are applied to a number of illustrative examples. While the main emphasis of the book is theoretical, descriptions of the experiments which have played a central role in the development of quantum optics are included.

A summary of the topics included in this text book is given as follows:

A familiarity with non-relativistic quantum mechanics is assumed. As we will be concerned with the quantum properties of light and its interaction with atoms, the electromagnetic field is quantised in the second chapter. Commonly used basis states for the field, the number states, the coherent states, and the squeezed state are introduced and their properties discussed. A definition of optical coherence is given via a set of field correlation functions in Chap. 3. Various representations for the electromagnetic field are introduced in Chap. 4 using the number states and the coherent states as a basis.

In Chap. 5 we present a number of simple models which illustrate some of the quantum correlation phenomena we discuss in later chapters. In Chap. 6 a rather lengthy description is given of the quantum theory of damping and the stochastic methods which may be employed to treat problems with damping. In Chap. 7 we present the input–output formulation of interactions in optical cavities. This theory plays a central role in the study of squeezed light generation. In Chap. 8 the input–output theory is applied to several systems in nonlinear optics, which produce squeezed light. Comparison with experiments is included. Applications of squeezed light in the field of optical interferometry are given. Potential use of squeezed light in gravitational wave interferometry is discussed.

In Chap. 9 two examples are given where the steady state quantum statistics of a field generated via a nonlinear optical interaction may be found exactly. In the case of parametric subharmonic generation the quantum tunnelling time between two states of a superposition is calculated.

In Chap. 10 we introduce atoms for the first time. The atomic energy levels are quantised and the interaction Hamiltonian between a two-level atom and the electromagnetic field derived. The spontaneous decay of an excited atom into a vacuum is treated. The modification of the atomic decay when the vacuum is squeezed, is also studied. In Chap. 11 we treat the classic problem of resonance fluorescence from a coherently driven atom. The resonance fluorescence spectrum is derived as is the photon antibunching of the emitted light. A comparison of theory with experimental results is given.

In Chap. 12 the quantum theory of the laser is developed including the theory of pump-noise-suppressed lasers, which give a sub-Poissonian output. In Chap. 13 a full quantum treatment is presented of optical bistability and four-wave mixing. Both systems involve the interaction of an ensemble of two-level atoms with a cavity field. The generation of squeezed light from these systems is analysed. Fundamental questions in quantum mechanics are addressed in Chap. 14. Experimental tests of the Bell inequalities in optics are described. In Chap. 15 quantum non-demolition measurements in optical systems are analysed. Further fundamentals of quantum coherence and the quantum measurement theory are discussed in Chap. 16.

In Chap. 17 an introduction to the newly emerging field of atomic optics is given.

2. Quantisation of the Electromagnetic Field

The study of the quantum features of light requires the quantisation of the electromagnetic field. In this chapter we quantise the field and introduce three possible sets of basis states, namely, the Fock or number states, the coherent states and the squeezed states. The properties of these states are discussed. The phase operator and the associated phase states are also introduced.

2.1 Field Quantisation

The major emphasis of this text is concerned with the uniquely quantum-mechanical properties of the electromagnetic field, which are not present in a classical treatment. As such we shall begin immediately by quantizing the electromagnetic field. We shall make use of an expansion of the vector potential for the electromagnetic field in terms of cavity modes. The problem then reduces to the quantization of the harmonic oscillator corresponding to each individual cavity mode.

We shall also introduce states of the electromagnetic field appropriate to the description of optical fields. The first set of states we introduce are the number states corresponding to having a definite number of photons in the field. It turns out that it is extremely difficult to create experimentally a number state of the field, though fields containing a very small number of photons have been generated. A more typical optical field will involve a superposition of number states. One such field is the coherent state of the field which has the minimum uncertainty in amplitude and phase allowed by the uncertainty principle, and hence is the closest possible quantum mechanical state to a classical field. It also possesses a high degree of optical coherence as will be discussed in Chap. 3, hence the name coherent state. The coherent state plays a fundamental role in quantum optics and has a practical significance in that a highly stabilized laser operating well above threshold generates a coherent state.

A rather more exotic set of states of the electromagnetic field are the squeezed states. These are also minimum-uncertainty states but unlike the coherent states the quantum noise is not uniformly distributed in phase. Squeezed states may have less noise in one quadrature than the vacuum. As a consequence the noise in the other quadrature is increased. We introduce the basic properties of squeezed states in this chapter. In Chap. 8 we describe ways to generate squeezed states and their applications.

While states of definite photon number are readily defined as eigenstates of the number operator a corresponding description of states of definite phase is more difficult. This is due to the problems involved in constructing a Hermitian phase operator to describe a bounded physical quantity like phase. How this problem may be resolved together with the properties of phase states is discussed in the final section of this chapter.

A convenient starting point for the quantisation of the electromagnetic field is the classical field equations. The free electromagnetic field obeys the source free Maxwell equations.

$$\nabla \cdot \boldsymbol{B} = 0 \ , \tag{2.1a}$$

$$\nabla \times \boldsymbol{E} = -\frac{\partial \boldsymbol{B}}{\partial t} \ , \tag{2.1b}$$

$$\nabla \cdot \boldsymbol{D} = 0 \ , \tag{2.1c}$$

$$\nabla \times \boldsymbol{H} = \frac{\partial \boldsymbol{D}}{\partial t} \ , \tag{2.1d}$$

where $\boldsymbol{B} = \mu_0 \boldsymbol{H}$, $\boldsymbol{D} = \varepsilon_0 \boldsymbol{E}$, μ_0 and ε_0 being the magnetic permeability and electric permittivity of free space, and $\mu_0 \varepsilon_0 = c^{-2}$. Maxwell's equations are gauge invariant when no sources are present. A convenient choice of gauge for problems in quantum optics is the Coulomb gauge. In the Coulomb gauge both $\boldsymbol{B}$ and $\boldsymbol{E}$ may be determined from a vector potential $\boldsymbol{A}(\boldsymbol{r}, t)$ as follows

$$\boldsymbol{B} = \nabla \times \boldsymbol{A} \ , \tag{2.2a}$$

$$\boldsymbol{E} = -\frac{\partial \boldsymbol{A}}{\partial t} \ , \tag{2.2b}$$

with the Coulomb gauge condition

$$\nabla \cdot \boldsymbol{A} = 0 \ . \tag{2.3}$$

Substituting (2.2a) into (2.1d) we find that $\boldsymbol{A}(\boldsymbol{r}, t)$ satisfies the wave equation

$$\nabla^2 \boldsymbol{A}(\boldsymbol{r}, t) = \frac{1}{c^2} \frac{\partial^2 \boldsymbol{A}(\boldsymbol{r}, t)}{\partial t^2} \ . \tag{2.4}$$

We separate the vector potential into two complex terms

$$\boldsymbol{A}(\boldsymbol{r}, t) = \boldsymbol{A}^{(+)}(\boldsymbol{r}, t) + \boldsymbol{A}^{(-)}(\boldsymbol{r}, t) \ , \tag{2.5}$$

where $\boldsymbol{A}^{(+)}(\boldsymbol{r}, t)$ contains all amplitudes which vary as $\mathrm{e}^{-\mathrm{i}\omega t}$ for $\omega > 0$ and $\boldsymbol{A}^{(-)}(\boldsymbol{r}, t)$ contains all amplitudes which vary as $\mathrm{e}^{\mathrm{i}\omega t}$ and $\boldsymbol{A}^{(-)} = (\boldsymbol{A}^{(+)})^*$.

It is more convenient to deal with a discrete set of variables rather than the whole continuum. We shall therefore describe the field restricted to a certain volume of space and expand the vector potential in terms of a discrete set of orthogonal mode functions:

$$A^{(+)}(r, t) = \sum_k c_k u_k(r) e^{-i\omega_k t} \;, \tag{2.6}$$

where the Fourier coefficients c_k are constant for a free field. The set of vector mode functions $u_k(r)$ which correspond to the frequency ω_k will satisfy the wave equation

$$\left(\nabla^2 + \frac{\omega_k^2}{c^2}\right) u_k(r) = 0 \tag{2.7}$$

provided the volume contains no refracting material. The mode functions are also required to satisfy the transversality condition,

$$\nabla \cdot u_k(r) = 0 \;. \tag{2.8}$$

The mode functions form a complete orthonormal set

$$\int_V u_k^*(r) u_{k'}(r) dr = \delta_{kk'} \;. \tag{2.9}$$

The mode functions depend on the boundary conditions of the physical volume under consideration, e.g., periodic boundary conditions corresponding to travelling-wave modes or conditions appropriate to reflecting walls which lead to standing waves. E.g., the plane wave mode functions appropriate to a cubical volume of side L may be written as

$$u_k(r) = L^{-3/2} \hat{e}^{(\lambda)} \exp(i k \cdot r) \tag{2.10}$$

where $\hat{e}^{(\lambda)}$ is the unit polarization vector. The mode index k describes several discrete variables, the polarisation index ($\lambda = 1, 2$) and the three Cartesian components of the propagation vector k. Each component of the wave vector k takes the values

$$k_x = \frac{2\pi n_x}{L}, \quad k_y = \frac{2\pi n_y}{L}, \quad k_z = \frac{2\pi n_z}{L}, \qquad n_x, n_y, n_z = 0, \pm 1, \pm 2, \ldots \tag{2.11}$$

The polarization vector $\hat{e}^{(\lambda)}$ is required to be perpendicular to k by the transversality condition (2.8).

The vector potential may now be written in the form

$$A(r, t) = \sum_k \left(\frac{\hbar}{2\omega_k \varepsilon_0}\right)^{1/2} [a_k u_k(r) e^{-i\omega_k t} + a_k^\dagger u_k^*(r) e^{i\omega_k t}] \;. \tag{2.12}$$

The corresponding form for the electric field is

$$E(r, t) = i \sum_k \left(\frac{\hbar\omega_k}{2\varepsilon_0}\right)^{1/2} [a_k u_k(r) e^{-i\omega_k t} - a_k^\dagger u_k^*(r) e^{i\omega_k t}] \;. \tag{2.13}$$

The normalization factors have been chosen such that the amplitudes a_k and $a_k^\dagger$ are dimensionless.

In classical electromagnetic theory these Fourier amplitudes are complex numbers. Quantisation of the electromagnetic field is accomplished by choosing a_k and $a_k^\dagger$ to be mutually adjoint operators. Since photons are bosons the appropriate commutation relations to choose for the operators a_k and $a_k^\dagger$ are the boson commutation relations

$$[a_k, a_{k'}] = [a_k^\dagger, a_{k'}^\dagger] = 0, \quad [a_k, a_{k'}^\dagger] = \delta_{kk'} \ . \tag{2.14}$$

The dynamical behaviour of the electric-field amplitudes may then be described by an ensemble of independent harmonic oscillators obeying the above commutation relations. The quantum states of each mode may now be discussed independently of one another. The state in each mode may be described by a state vector $|\Psi\rangle_k$ of the Hilbert space appropriate to that mode. The states of the entire field are then defined in the tensor product space of the Hilbert spaces for all of the modes.

The Hamiltonian for the electromagnetic field is given by

$$H = \frac{1}{2}\int (\varepsilon_0 \boldsymbol{E}^2 + \mu_0 \boldsymbol{H}^2) d\boldsymbol{r} \ . \tag{2.15}$$

Substituting (2.13) for $\boldsymbol{E}$ and the equivalent expression for $\boldsymbol{H}$ and making use of the conditions (2.8) and (2.9), the Hamiltonian may be reduced to the form

$$H = \sum_k \hbar\omega_k (a_k^\dagger a_k + \tfrac{1}{2}) \ . \tag{2.16}$$

This represents the sum of the number of photons in each mode multiplied by the energy of a photon in that mode, plus $\frac{1}{2}\hbar\omega_k$ representing the energy of the vacuum fluctuations in each mode. We shall now consider three possible representations of the electromagnetic field.

2.2 Fock or Number States

The Hamiltonian (2.15) has the eigenvalues $h\omega_k(n_k + \frac{1}{2})$ where n_k is an integer ($n_k = 0, 1, 2, \ldots, \infty$). The eigenstates are written as $|n_k\rangle$ and are known as number or Fock states. They are eigenstates of the number operator $N_k = a_k^\dagger a_k$

$$a_k^\dagger a_k |n_k\rangle = n_k |n_k\rangle \ . \tag{2.17}$$

The ground state of the oscillator (or vacuum state of the field mode) is defined by

$$a_k |0\rangle = 0 \ . \tag{2.18}$$

From (2.16 and 18) we see that the energy of the ground state is given by

$$\langle 0|H|0\rangle = \frac{1}{2}\sum_k \hbar\omega_k \ . \tag{2.19}$$

Since there is no upper bound to the frequencies in the sum over electromagnetic field modes, the energy of the ground state is infinite, a conceptual difficulty of quantized radiation field theory. However, since practical experiments measure a change in the total energy of the electromagnetic field the infinite zero-point energy does not lead to any divergence in practice. Further discussions on this point may be found in [2.1]. a_k and $a_k^\dagger$ are raising and lowering operators for the harmonic oscillator ladder of eigenstates. In terms of photons they represent the annihilation and creation of a photon with the wave vector $\boldsymbol{k}$ and a polarisation $\hat{e}_k$. Hence the terminology, annihilation and creation operators. Application of the creation and annihilation operators to the number states yield

$$a_k|n_k\rangle = n_k^{1/2}|n_k - 1\rangle, \quad a_k^\dagger|n_k\rangle = (n_k+1)^{1/2}|n_k+1\rangle \ . \tag{2.20}$$

The state vectors for the higher excited states may be obtained from the vacuum by successive application of the creation operator

$$|n_k\rangle = \frac{(a_k^\dagger)^{n_k}}{(n_k!)^{1/2}}|0\rangle, \quad n_k = 0, 1, 2 \ldots \ . \tag{2.21}$$

The number states are orthogonal

$$\langle n_k|m_k\rangle = \delta_{mn} \ , \tag{2.22}$$

and complete

$$\sum_{n_k=0}^{\infty} |n_k\rangle\langle n_k| = 1 \ . \tag{2.23}$$

Since the norm of these eigenvectors is finite, they form a complete set of basis vectors for a Hilbert space.

While the number states form a useful representation for high-energy photons, e.g. γ rays where the number of photons is very small, they are not the most suitable representation for optical fields where the total number of photons is large. Experimental difficulties have prevented the generation of photon number states with more than a small number of photons. Most optical fields are either a superposition of number states (pure state) or a mixture of number states (mixed state). Despite this the number states of the electromagnetic field have been used as a basis for several problems in quantum optics including some laser theories.

2.3 Coherent States

A more appropriate basis for many optical fields are the coherent states [2.2]. The coherent states have an indefinite number of photons which allows them to have a more precisely defined phase than a number state where the phase is completely random. The product of the uncertainty in amplitude and phase for a coherent state is the minimum allowed by the uncertainty principle. In this sense they are the closest quantum mechanical states to a classical description of the field. We shall outline the basic properties of the coherent states below. These states are most easily generated using the unitary displacement operator

$$D(\alpha) = \exp(\alpha a^\dagger - \alpha^* a) \ , \tag{2.24}$$

where α is an arbitrary complex number.

Using the operator theorem [2.2]

$$\mathrm{e}^{A+B} = \mathrm{e}^{A}\mathrm{e}^{B}\mathrm{e}^{-[A,\,B]/2} \ , \tag{2.25}$$

which holds when

$$[A, [A, B]] = [B, [A, B]] = 0 \ ,$$

we can write $D(\alpha)$ as

$$D(\alpha) = \mathrm{e}^{-|\alpha|^2/2}\mathrm{e}^{\alpha a^\dagger}\mathrm{e}^{-\alpha^* a} \ . \tag{2.26}$$

The displacement operator $D(\alpha)$ has the following properties

$$D^\dagger(\alpha) = D^{-1}(\alpha) = D(-\alpha), \qquad D^\dagger(\alpha) a D(\alpha) = a + \alpha \ ,$$

$$D^\dagger(\alpha)\, a^\dagger D(\alpha) = a^\dagger + \alpha^* \ . \tag{2.27}$$

The coherent state $|\alpha\rangle$ is generated by operating with $D(\alpha)$ on the vacuum state

$$|\alpha\rangle = D(\alpha)|0\rangle \ . \tag{2.28}$$

The coherent states are eigenstates of the annihilation operator a. This may be proved as follows:

$$D^\dagger(\alpha) a |\alpha\rangle = D^\dagger(\alpha) a D(\alpha)|0\rangle = (a + \alpha)|0\rangle = \alpha|0\rangle \ . \tag{2.29}$$

Multiplying both sides by $D(\alpha)$ we arrive at the eigenvalue equation

$$a|\alpha\rangle = \alpha|\alpha\rangle \ . \tag{2.30}$$

Since a is a non-Hermitian operator its eigenvalues α are complex.

Another useful property which follows using (2.25) is

$$D(\alpha + \beta) = D(\alpha)D(\beta)\exp(-\mathrm{i}\,\mathrm{Im}\{\alpha\beta^*\}) \ . \tag{2.31}$$

The coherent states contain an indefinite number of photons. This may be made apparent by considering an expansion of the coherent states in the number-states basis.

Taking the scalar product of both sides of (2.30) with $\langle n|$ we find the recursion relation

$$(n+1)^{1/2}\langle n+1|\alpha\rangle = \alpha\langle n|\alpha\rangle \ . \tag{2.32}$$

It follows that

$$\langle n|\alpha\rangle = \frac{\alpha^n}{(n!)^{1/2}}\langle 0|\alpha\rangle \ . \tag{2.33}$$

We may expand $|\alpha\rangle$ in terms of the number states $|n\rangle$ with expansion coefficients $\langle n|\alpha\rangle$ as follows

$$|\alpha\rangle = \sum |n\rangle\langle n|\alpha\rangle = \langle 0|\alpha\rangle \sum_n \frac{\alpha^n}{(n!)^{1/2}}|n\rangle \ . \tag{2.34}$$

The squared length of the vector $|\alpha\rangle$ is thus

$$|\langle\alpha|\alpha\rangle|^2 = |\langle 0|\alpha\rangle|^2 \sum_n \frac{|\alpha|^{2n}}{n!} = |\langle 0|\alpha\rangle|^2\, \mathrm{e}^{|\alpha|^2} \ . \tag{2.35}$$

It is easily seen that

$$\begin{aligned}\langle 0|\alpha\rangle &= \langle 0|D(\alpha)|0\rangle \\ &= \mathrm{e}^{-|\alpha|^2/2} \ .\end{aligned} \tag{2.36}$$

Thus $|\langle\alpha|\alpha\rangle|^2 = 1$ and the coherent states are normalized.

The coherent state may then be expanded in terms of the number states as

$$|\alpha\rangle = \mathrm{e}^{-|\alpha|^2/2} \sum \frac{\alpha^n}{(n!)^{1/2}}|n\rangle \ . \tag{2.37}$$

We note that the probability distribution of photons in a coherent state is a Poisson distribution

$$P(n) = |\langle n|\alpha\rangle|^2 = \frac{|\alpha|^{2n}\mathrm{e}^{-|\alpha|^2}}{n!} \ , \tag{2.38}$$

where $|\alpha|^2$ is the mean number of photons ($\bar{n} = \langle\alpha|a^\dagger a|\alpha\rangle = |\alpha|^2$).

The scalar product of two coherent states is

$$\langle\beta|\alpha\rangle = \langle 0|D^+(\beta)D(\alpha)|0\rangle \ . \tag{2.39}$$

Using (2.26) this becomes

$$\langle\beta|\alpha\rangle = \exp[-\tfrac{1}{2}(|\alpha|^2 + |\beta|^2) + \alpha\beta^*] \ . \tag{2.40}$$

The absolute magnitude of the scalar product is

$$|\langle\beta|\alpha\rangle|^2 = \mathrm{e}^{-|\alpha-\beta|^2} \ . \tag{2.41}$$

Thus the coherent states are not orthogonal although two states $|\alpha\rangle$ and $|\beta\rangle$ become approximately orthogonal in the limit $|\alpha - \beta| \gg 1$. The coherent states form a two-dimensional continuum of states and are, in fact, overcomplete. The completeness relation

$$\frac{1}{\pi}\int |\alpha\rangle\langle\alpha|\,d^2\alpha = 1 \ , \tag{2.42}$$

may be proved as follows.

We use the expansion (2.37) to give

$$\int |\alpha\rangle\langle\alpha|\frac{d^2\alpha}{\pi} = \sum_{n=0}^{\infty}\sum_{m=0}^{\infty}\frac{|n\rangle\langle m|}{\pi\sqrt{n!\,m!}}\int e^{-|\alpha|^2}\alpha^{*m}\alpha^n\,d^2\alpha \ . \tag{2.43}$$

Changing to polar coordinates this becomes

$$\int |\alpha\rangle\langle\alpha|\frac{d^2\alpha}{\pi} = \sum_{n,m=0}^{\infty}\frac{|n\rangle\langle m|}{\pi\sqrt{n!\,m!}}\int_0^{\infty} r\,dr\,e^{-r^2}r^{n+m}\int_0^{2\pi} d\theta\,e^{i(n-m)\theta} \ . \tag{2.44}$$

Using

$$\int_0^{2\pi} d\theta\,e^{i(n-m)\theta} = 2\pi\delta_{nm} \ , \tag{2.45}$$

we have

$$\int |\alpha\rangle\langle\alpha|\frac{d^2\alpha}{\pi} = \sum_{n=0}^{\infty}\frac{|n\rangle\langle n|}{n!}\int_0^{\infty} d\varepsilon\,e^{-\varepsilon}\varepsilon^n \ , \tag{2.46}$$

where we let $\varepsilon = r^2$. The integral equals $n!$. Hence we have

$$\int |\alpha\rangle\langle\alpha|\frac{d^2\alpha}{\pi} = \sum_{n=0}^{\infty}|n\rangle\langle n| = 1 \ , \tag{2.47}$$

following from the completeness relation for the number states.

An alternative proof of the completeness of the coherent states may be given as follows. Using the relation [2.3]

$$e^{\zeta B}A\,e^{-\zeta B} = A + \zeta[B,A] + \frac{\zeta^2}{2!}[B,[B,A]] + \cdots \ , \tag{2.48}$$

it is easy to see that all the operators A such that

$$D^\dagger(\alpha)AD(\alpha) = A \tag{2.49}$$

are proportional to the identity.

We consider

$$A = \int d^2\alpha \,|\alpha\rangle\langle\alpha|$$

then

$$D^\dagger(\beta)\int d^2\alpha|\alpha\rangle\langle\alpha|D(\beta) = \int d^2\alpha|\alpha-\beta\rangle\langle\alpha-\beta| = \int d^2\alpha|\alpha\rangle\langle\alpha| \ . \qquad (2.50)$$

Then using the above result we conclude that

$$\int d^2\alpha|\alpha\rangle\langle\alpha| \propto I \ . \qquad (2.51)$$

The constant of proportionality is easily seen to be π.

The coherent states have a physical significance in that the field generated by a highly stabilized laser operating well above threshold is a coherent state. They form a useful basis for expanding the optical field in problems in laser physics and nonlinear optics. The coherence properties of light fields and the significance of the coherent states will be discussed in Chap. 3.

2.4 Squeezed States

A general class of minimum-uncertainty states are known as *squeezed states*. In general, a squeezed state may have less noise in one quadrature than a coherent state. To satisfy the requirements of a minimum-uncertainty state the noise in the other quadrature is greater than that of a coherent state. The coherent states are a particular member of this more general class of minimum uncertainty states with equal noise in both quadratures. We shall begin our discussion by defining a family of minimum-uncertainty states. Let us calculate the variances for the position and momentum operators for the harmonic oscillator

$$q = \sqrt{\frac{\hbar}{2\omega}}(a + a^\dagger), \qquad p = \mathrm{i}\sqrt{\frac{\hbar\omega}{2}}(a - a^\dagger) \ . \qquad (2.52)$$

The variances are defined by

$$V(A) = (\Delta A)^2 = \langle A^2\rangle - \langle A\rangle^2 \ . \qquad (2.53)$$

In a coherent state we obtain

$$(\Delta q)^2_{\mathrm{coh}} = \frac{\hbar}{2\omega}, \qquad (\Delta p)^2_{\mathrm{coh}} = \frac{\hbar\omega}{2} \ . \qquad (2.54)$$

Thus the product of the uncertainties is a minimum

$$(\Delta p\,\Delta q)_{\mathrm{coh}} = \frac{\hbar}{2} \ . \qquad (2.55)$$

Thus, there exists a sense in which the description of the state of an oscillator by a coherent state represents as close an approach to classical localisation as possible. We shall consider the properties of a single-mode field. We may write the annihilation operator a as a linear combination of two Hermitian operators

$$a = \frac{X_1 + \mathrm{i}X_2}{2} \ . \tag{2.56}$$

X_1 and X_2, the real and imaginary parts of the complex amplitude, give dimensionless amplitudes for the modes' two quadrature phases. They obey the following commutation relation

$$[X_1, X_2] = 2i \ . \tag{2.57}$$

The corresponding uncertainty principle is

$$\Delta X_1 \Delta X_2 \geq 1 \ . \tag{2.58}$$

This relation with the equals sign defines a family of minimum-uncertainty states. The coherent states are a particular minimum-uncertainty state with

$$\Delta X_1 = \Delta X_2 = 1 \ . \tag{2.59}$$

The coherent state $|\alpha\rangle$ has the mean complex amplitude α and it is a minimum-uncertainty state for X_1 and X_2, with equal uncertainties in the two quadrature phases. A coherent state may be represented by an "error circle" in a complex amplitude plane whose axes are X_1 and X_2 (Fig. 2.1a). The centre of the error circle lies at $\frac{1}{2}\langle X_1 + \mathrm{i}X_2\rangle = \alpha$ and the radius $\Delta X_1 = \Delta X_2 = 1$ accounts for the uncertainties in X_1 and X_2.

There is obviously a whole family of minimum-uncertainty states defined by $\Delta X_1 \Delta X_2 = 1$. If we plot ΔX_1 against ΔX_2 the minimum-uncertainty states lie on a hyperbola (Fig. 2.2). Only points lying to the right of this hyperbola correspond to physical states. The coherent state with $\Delta X_1 = \Delta X_2$ is a special case of a more general class of states which may have reduced uncertainty in one quadrature at the expense of increased uncertainty in the other ($\Delta X_1 < 1 < \Delta X_2$). These states correspond to the shaded region in Fig. 2.2. Such states we shall call *squeezed states* [2.4]. They may be generated by using the unitary squeeze operator [2.5]

$$S(\varepsilon) = \exp(1/2\varepsilon^* a^2 - 1/2\varepsilon a^{\dagger 2}) \ , \tag{2.60}$$

where $\varepsilon = re^{2i\phi}$.

Note the squeeze operator obeys the relations

$$S^\dagger(\varepsilon) = S^{-1}(\varepsilon) = S(-\varepsilon) \ , \tag{2.61}$$

and has the following useful transformation properties

$$\begin{aligned} S^\dagger(\varepsilon) a S(\varepsilon) &= a \cosh r - a^\dagger \mathrm{e}^{-2\mathrm{i}\phi} \sinh r \ , \\ S^\dagger(\varepsilon) a^\dagger S(\varepsilon) &= a^\dagger \cosh r - a \mathrm{e}^{2\mathrm{i}\phi} \sinh r \ , \\ S^\dagger(\varepsilon)(Y_1 + \mathrm{i}Y_2) S(\varepsilon) &= Y_1 \mathrm{e}^{-r} + \mathrm{i}Y_2 \mathrm{e}^{r} \ , \end{aligned} \tag{2.62}$$

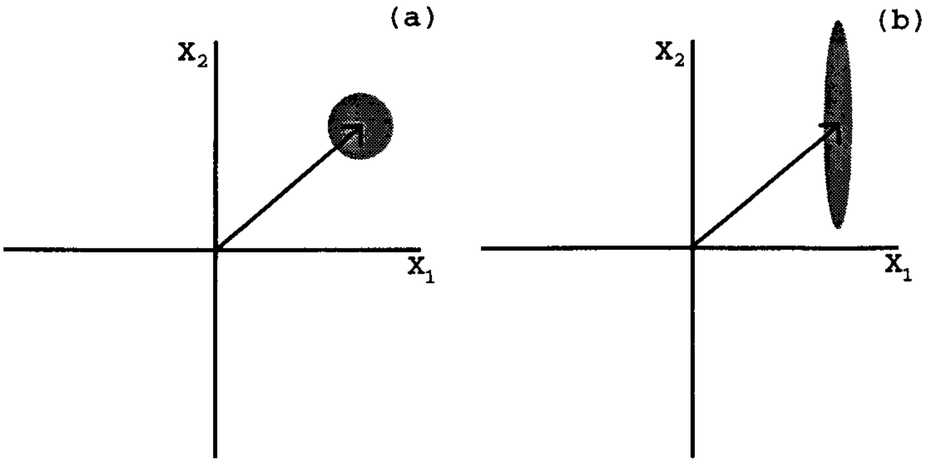

Fig. 2.1. Phase-space plot showing the uncertainty in (a) a coherent state $|\alpha\rangle$, and (b) a squeezed state $|\alpha, r\rangle$

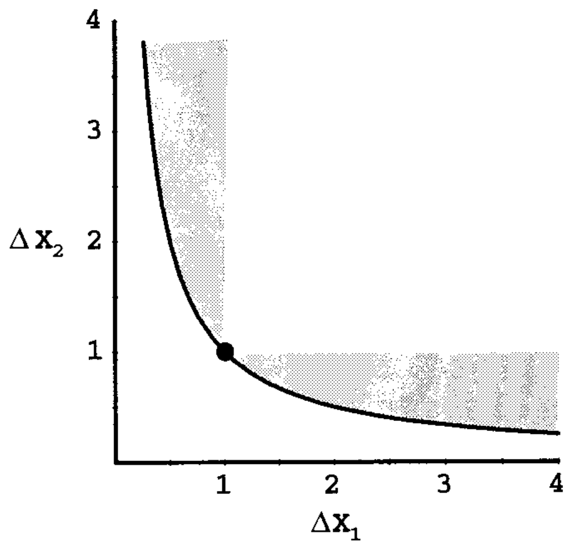

Fig. 2.2. Plot of ΔX_1 versus ΔX_2 for the minimum-uncertainty states. The dot marks a coherent state while the shaded region corresponds to the squeezed states

where

$$Y_1 + \mathrm{i} Y_2 = (X_1 + \mathrm{i} X_2)\mathrm{e}^{-\mathrm{i}\phi} \tag{2.63}$$

is a rotated complex amplitude. The squeeze operator attenuates one component of the (rotated) complex amplitude, and it amplifies the other component. The degree of attenuation and amplification is determined by $r = |\varepsilon|$, which will be called the *squeeze factor*. The squeezed state $|\alpha, \varepsilon\rangle$ is obtained by first squeezing the vacuum and then displacing it

$$|\alpha, \varepsilon\rangle = D(\alpha) S(\varepsilon) |0\rangle \ . \tag{2.64}$$

A squeezed state has the following expectation values and variances

$$\begin{aligned}
&\langle X_1 + \mathrm{i}X_2 \rangle = \langle Y_1 + \mathrm{i}\,Y_2 \rangle \mathrm{e}^{\mathrm{i}\phi} = 2\alpha \ , \\
&\Delta Y_1 = \mathrm{e}^{-r}, \qquad \Delta Y_2 = \mathrm{e}^{r} \ , \\
&\langle N \rangle = |\alpha|^2 + \sinh^2 r \ , \\
&(\Delta N)^2 = |\alpha \cosh r - \alpha^* \mathrm{e}^{2\mathrm{i}\phi} \sinh r|^2 + 2\cosh^2 r \sinh^2 r \ .
\end{aligned} \tag{2.65}$$

Thus the squeezed state has unequal uncertainties for Y_1 and Y_2 as seen in the error ellipse shown in Fig. 2.1b. The principal axes of the ellipse lie along the Y_1 and Y_2 axes, and the principal radii are ΔY_1 and ΔY_2. A more rigorous definition of these error ellipses as contours of the Wigner function is given in Chap. 3.

2.5 Two-Photon Coherent States

We may define squeezed states in an alternative but equivalent way [2.6]. As this definition is sometimes used in the literature we include it for completeness.

Consider the operator

$$b = \mu a + \nu a^\dagger \tag{2.66}$$

where

$$|\mu|^2 - |\nu|^2 = 1 \ .$$

Then b obeys the commutation relation

$$[b, b^\dagger] = 1 \ . \tag{2.67}$$

We may write (2.66) as

$$b = UaU^\dagger \tag{2.68}$$

where U is a unitary operator. The eigenstates of b have been called *two-photon coherent states* and are closely related to the squeezed states.

The eigenvalue equation may be written as

$$b|\beta\rangle_{\mathrm{g}} = \beta|\beta\rangle_{\mathrm{g}} \ . \tag{2.69}$$

From (2.68) it follows that

$$|\beta\rangle_{\mathrm{g}} = U|\beta\rangle \tag{2.70}$$

where $|\beta\rangle$ are the eigenstates of a.

The properties of $|\beta\rangle_{\mathrm{g}}$ may be proved to parallel those of the coherent states. The state $|\beta\rangle_{\mathrm{g}}$ may be obtained by operating on the vacuum

$$|\beta\rangle_{\mathrm{g}} = D_{\mathrm{g}}(\beta)|0\rangle_{\mathrm{g}} \tag{2.71}$$

with the displacement operator

$$D_g(\beta) = e^{\beta b^\dagger - \beta^* b} \tag{2.72}$$

and $|0\rangle_g = U|0\rangle$. The two-photon coherent states are complete

$$\int |\beta\rangle_{g\,g}\langle\beta| \frac{d^2\beta}{\pi} = 1 \tag{2.73}$$

and their scalar product is

$$_g\langle\beta|\beta'\rangle_g = \exp(\beta^*\beta' - \tfrac{1}{2}|\beta|^2 - \tfrac{1}{2}|\beta'|^2) \ . \tag{2.74}$$

We now consider the relation between the two-photon coherent states and the squeezed states as previously defined. We first note that

$$U \equiv S(\varepsilon)$$

with $\mu = \cosh r$ and $\nu = e^{2i\phi} \sinh r$. Thus

$$|0\rangle_g \equiv |0, \varepsilon\rangle \tag{2.75}$$

with the above relations between (μ, ν) and (r, θ). Using this result in (2.71) and rewriting the displacement operator, $D_g(\beta)$, in terms of a and $a^\dagger$ we find

$$|\beta\rangle_g = D(\alpha)S(\varepsilon)|0\rangle = |\alpha, \varepsilon\rangle \tag{2.76}$$

where

$$\alpha = \mu\beta - \nu\beta^* \ .$$

Thus we have found the equivalent squeezed state for the given two-photon coherent state.

Finally, we note that the two-photon coherent state $|\beta\rangle_g$ may be written as

$$|\beta\rangle_g = S(\varepsilon)D(\beta)|0\rangle \ .$$

Thus the two-photon coherent state is generated by first displacing the vacuum state, then squeezing. This is the opposite procedure to that which defines the squeezed state $|\alpha, \varepsilon\rangle$. The two procedures yield the same state if the displacement parameters α and β are related as discussed above.

The completeness relation for the two-photon coherent states may be employed to derive the completeness relation for the squeezed states. Using the above results we have

$$\int \frac{d^2\beta}{\pi} |\beta\cosh r - \beta^* e^{2i\phi}\sinh r, \varepsilon\rangle\langle\beta\cosh r - \beta^* e^{2i\phi}\sinh r, \varepsilon| = 1 \ . \tag{2.77}$$

The change of variable

$$\alpha = \beta\cosh r - \beta^* e^{2i\phi} \sinh r \tag{2.78}$$

leaves the measure invariant, that is $d^2\alpha = d^2\beta$. Thus

$$\int \frac{d^2\alpha}{\pi} |\alpha, \varepsilon\rangle\langle\alpha, \varepsilon| = 1 \; . \tag{2.79}$$

2.6 Variance in the Electric Field

The electric field for a single mode may be written in terms of the operators X_1 and X_2 as

$$E(\boldsymbol{r}, t) = \frac{1}{\sqrt{L^3}} \left(\frac{\hbar\omega}{2\varepsilon_0}\right)^{1/2} [X_1 \sin(\omega t - \boldsymbol{k}\cdot\boldsymbol{r}) - X_2 \cos(\omega t - \boldsymbol{k}\cdot\boldsymbol{r})] \; . \tag{2.80}$$

The variance in the electric field is given by

$$\begin{aligned} V(E(\boldsymbol{r}, t)) = K\{ & V(X_1)\sin^2(\omega t - \boldsymbol{k}\cdot\boldsymbol{r}) + V(X_2)\cos^2(\omega t - \boldsymbol{k}\cdot\boldsymbol{r}) \\ & - \sin[2(\omega t - \boldsymbol{k}\cdot\boldsymbol{r})]\, V(X_1, X_2)\} \end{aligned} \tag{2.81}$$

where

$$K = \frac{1}{L^3}\left(\frac{2\hbar\omega}{\varepsilon_0}\right) ,$$

$$V(X_1, X_2) = \frac{\langle (X_1 X_2) + (X_2 X_1)\rangle}{2} - \langle X_1\rangle\langle X_2\rangle \; .$$

For a minimum-uncertainty state

$$V(X_1, X_2) = 0 \; . \tag{2.82}$$

Hence (2.81) reduces to

$$V(E(\boldsymbol{r}, t)) = K[V(X_1)\sin^2(\omega t - \boldsymbol{k}\cdot\boldsymbol{r}) + V(X_2)\cos^2(\omega t - \boldsymbol{k}\cdot\boldsymbol{r})] \; . \tag{2.83}$$

The mean and uncertainty of the electric field is exhibited in Figs. 2.3a–c where the line is thickened about a mean sinusoidal curve to represent the uncertainty in the electric field.

The variance of the electric field for a coherent state is a constant with time (Fig. 2.3a). This is due to the fact that while the coherent-state-error circle rotates about the origin at frequency ω, it has a constant projection on the axis defining the electric field. Whereas for a squeezed state the rotation of the error ellipse leads to a variance that oscillates with frequency 2ω. In Fig. 2.3b the coherent excitation appears in, the quadrature that has reduced noise. In Fig. 2.3c the coherent excitation appears in the quadrature with increased noise. This situation corresponds to the phase states discussed in [2.7] and in the final section of this chapter.

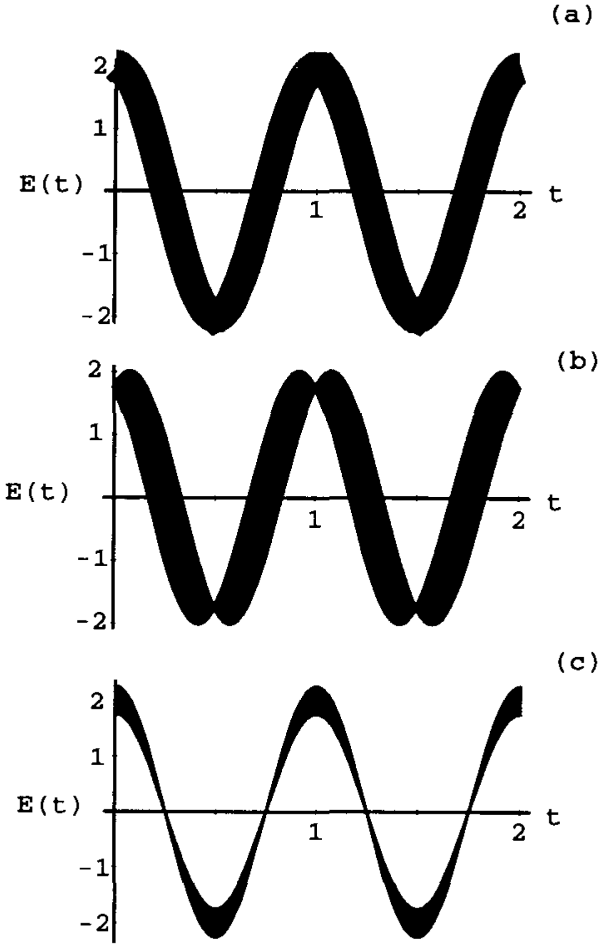

Fig. 2.3. Plot of the electric field versus time showing schematically the uncertainty in phase and amplitude for (a) a coherent state, (b) a squeezed state with reduced amplitude fluctuations, and (c) a squeezed state with reduced phase fluctuations

The squeezed state $|\alpha, r\rangle$ has the photon number distribution [2.6]

$$P(n) = (n!\mu)^{-1}\left(\frac{\nu}{2\mu}\right)^n \left|H_n\left(\frac{\beta}{\sqrt{2\mu\nu}}\right)\right|^2 e^{-|\beta|^2 + \frac{\nu}{2\mu}\beta^2 + \frac{\nu^*}{2\mu}\beta^{*2}} \tag{2.84}$$

where

$$\nu = \sinh r\, e^{2i\phi}, \qquad \mu = \cosh r, \qquad \beta = \mu\alpha + \nu\alpha^* .$$

$H_n(x)$ are Hermite polynomials.

The photon number distribution for a squeezed state may be broader or narrower than a Poissonian depending on whether the reduced fluctuations occur in the phase (X_2) or amplitude (X_1) component of the field. This is illustrated in Fig. 2.4a where we plot $P(n)$ for $r = 0$, $r > 0$, and $r < 0$. Note, a squeezed vacuum ($\alpha = 0$) contains only even numbers of photons since $H_n(0) = 0$ for n odd.

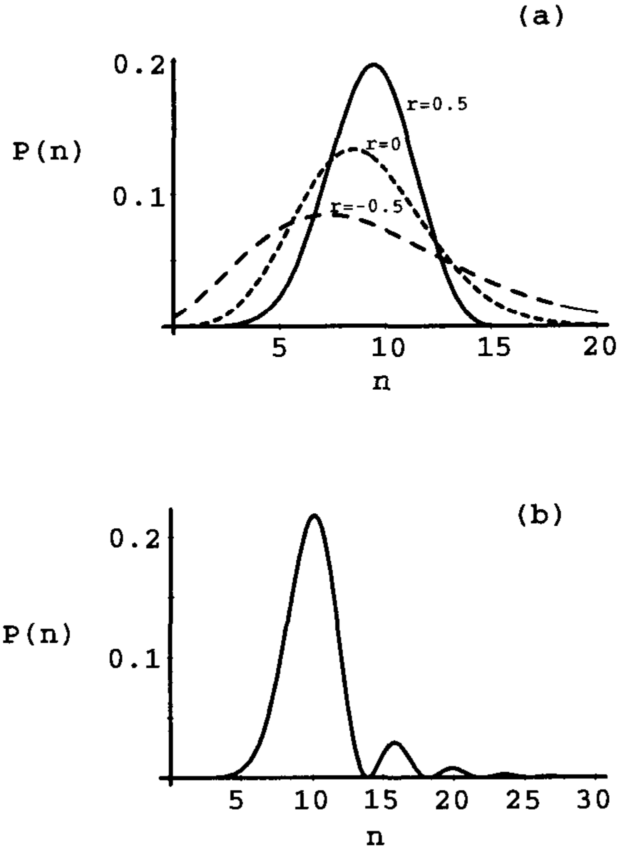

Fig. 2.4. Photon number distribution for a squeezed state $|\alpha, r\rangle$: (a) $\alpha = 3$, $r = 0, 0.5, -0.5$, (b) $\alpha = 3$, $r = 1.0$

For larger values of the squeeze parameter r, the photon number distribution exhibits oscillations, as depicted in Fig. 2.4b. These oscillations have been interpreted as interference in phase space [2.8].

2.7 Multimode Squeezed States

Multimode squeezed states are important since several devices produce light which is correlated at the two frequencies ω_+ and ω_-. Usually these frequencies are symmetrically placed either side of a carrier frequency. The squeezing exists not in the single modes but in the correlated state formed by the two modes.

A two-mode squeezed state may be defined by [2.9]

$$|\alpha_+, \alpha_-\rangle = D_+(\alpha_+)D_-(\alpha_-)S(G)|0\rangle \tag{2.85}$$

where the displacement operator is

$$D_\pm(\alpha) = \exp(\alpha a_\pm^\dagger - \alpha^* a_\pm) \ , \tag{2.86}$$

and the unitary two-mode squeeze operator is

$$S(G) = \exp(G^* a_+ a_- - G a_+^\dagger a_-^\dagger) \ . \tag{2.87}$$

The squeezing operator transforms the annihilation operators as

$$S^\dagger(G) a_\pm \, S(G) = a_\pm \cosh r - a_\mp^\dagger \, e^{i\theta} \sinh r \ , \tag{2.88}$$

where $G = re^{i\theta}$.

This gives for the following expectation values

$$\begin{aligned}
&\langle a_+ \rangle = \alpha_+ , \qquad \langle a_- \rangle = \alpha_- , \\
&\langle a_\pm^\dagger \, a_\pm \rangle = |\alpha_\pm|^2 + \sinh^2 r, \qquad \langle a_\pm^\dagger \, a_\mp^\dagger \rangle = \alpha_\pm^* \, \alpha_\mp , \\
&\langle a_\pm \, a_\pm \rangle = \alpha_\pm^2 , \qquad \langle a_+ a_- \rangle = \langle a_- a_+ \rangle = \alpha_+ \alpha_- - e^{i\theta} \sinh r \cosh r \ .
\end{aligned} \tag{2.89}$$

The quadrature operator X is generalized in the two-mode case to

$$X = \frac{1}{\sqrt{2}} (a_+ + a_+^\dagger + a_- + a_-^\dagger) \ . \tag{2.90}$$

As will be seen in Chap. 5, this definition is a particular case of a more general definition. It corresponds to the degenerate situation in which the frequencies of the two modes are equal.

The mean and variance of X in a two-mode squeezed state is

$$\begin{aligned}
&\langle X \rangle = 2(\mathrm{Re}\{\alpha_+\} + \mathrm{Re}\{\alpha_-\}) \ , \\
&V(X) = \left(e^{-2r} \cos^2 \frac{\theta}{2} + e^{2r} \sin^2 \frac{\theta}{2} \right) \ .
\end{aligned} \tag{2.91}$$

These results for two-mode squeezed states will be used in the analyses of nondegenerate parametric oscillation given in Chaps. 4 and 6.

2.8 Phase Properties of the Field

The definition of an Hermitian phase operator corresponding to the physical phase of the field has long been a problem. Initial attempts by P. Dirac led to a non-Hermitian operator with incorrect commutation relations. Many of these difficulties were made quite explicit in the work of *Susskind* and *Glogower* [2.10]. Recently, *Pegg* and *Barnett* [2.11] showed how to construct an Hermitian phase operator, the eigenstates of which, in an appropriate limit, generate the correct phase statistics for arbitrary states. We will first discuss the *Susskind–Glogower* (SG) phase operator.

Let a be the annihilation operator for a harmonic oscillator, representing a single field mode. In analogy with the classical polar decomposition of a complex amplitude we define the SG phase operator,

$$e^{i\phi} = (aa^{\dagger})^{-1/2}a \ . \tag{2.92}$$

The operator $e^{i\phi}$ has the number state expansion

$$e^{i\phi} = \sum_{n=0}^{\infty} |n\rangle\langle n+1| \tag{2.93}$$

and eigenstates $|e^{i\phi}\rangle$ like

$$|e^{i\phi}\rangle = \sum_{n=0}^{\infty} e^{in\phi}|n\rangle \quad \text{for} \quad -\pi < \phi \leq \pi \ . \tag{2.94}$$

It is easy to see from (2.93) that $e^{i\phi}$ is not unitary,

$$[e^{i\phi}, (e^{i\phi})^{\dagger}] = |0\rangle\langle 0| \ . \tag{2.95}$$

An equivalent statement is that the SG phase operator is not Hermitian. As an immediate consequence the eigenstates $|e^{i\phi}\rangle$ are not orthogonal. In many ways this is similar to the non-orthogonal eigenstates of the annihilation operator a, i.e. the coherent states. None-the-less these states do provide a resolution of identity

$$\int_{-\pi}^{\pi} d\phi \, |e^{i\phi}\rangle\langle e^{i\phi}| = 2\pi \ . \tag{2.96}$$

The phase distribution over the window $-\pi < \phi \leq \pi$ for any state $|\psi\rangle$ is then defined by

$$P(\phi) = \frac{1}{2\pi}|\langle e^{i\phi}|\psi\rangle|^2 \ . \tag{2.97}$$

The normalisation integral is

$$\int_{-\pi}^{\pi} P(\phi)d\phi = 1 \ . \tag{2.98}$$

The question arises; does this distribution correspond to the statistics of any physical phase measurement? At the present time there does not appear to be an answer. However, there are theoretical grounds [2.12] for believing that $P(\phi)$ is the correct distribution for optimal phase measurements. If this is accepted then the fact that the SG phase operator is not Hermitian is nothing to be concerned about. However, as we now show, one can define an Hermitian phase operator, the measurement statistics of which converge, in an appropriate limit, to the phase distribution of (2.97) [2.13].

Consider the state $|\phi_0\rangle$ defined on a finite subspace of the oscillator Hilbert space by

$$|\phi_0\rangle = (s+1)^{-1/2} \sum_{n=0}^{s} e^{in\phi_0}|n\rangle \ . \tag{2.99}$$

It is easy to demonstrate that the states $|\phi\rangle$ with the values of ϕ differing from ϕ_0 by integer multiples of $2\pi/(s+1)$ are orthogonal. Explicitly, these states are

$$|\phi_m\rangle = \exp\left(i\frac{a^\dagger a\, m\, 2\pi}{s+1}\right)|\phi_0\rangle; \quad m = 0, 1, \dots, s \ , \tag{2.100}$$

with

$$\phi_m = \phi_0 + \frac{2\pi m}{s+1} \ .$$

Thus $\phi_0 \leq \phi_m < \phi_0 + 2\pi$. In fact, these states form a complete orthonormal set on the truncated $(s+1)$ dimensional Hilbert space. We now construct the *Pegg–Barnett* (*PB*) Hermitian phase operator

$$\phi = \sum_{m=0}^{s} \phi_m |\phi_m\rangle\langle\phi_m| \ . \tag{2.101}$$

For states restricted to the truncated Hilbert space the measurement statistics of ϕ are given by the discrete distribution

$$P_m = |\langle\phi_m|\psi\rangle_s|^2 \tag{2.102}$$

where $|\psi\rangle_s$ is any vector of the truncated space.

It would seem natural now to take the limit $s \to \infty$ and recover an Hermitian phase operator on the full Hilbert space. However, in this limit the PB phase operator does not converge to an Hermitian phase operator, but the distribution in (2.102) does converge to the SG phase distribution in (2.97). To see this, choose $\phi_0 = 0$.

Then

$$P_m = (s+1)^{-1}\left|\sum_{n=0}^{s} \exp\left(-i\frac{nm\,2\pi}{s+1}\right)\psi_n\right|^2 \tag{2.103}$$

where $\psi_n = \langle n|\psi\rangle_s$.

As ϕ_m are uniformly distributed over 2π we define the probability density by

$$P(\phi) = \lim_{s\to\infty}\left[\left(\frac{2\pi}{s+1}\right)^{-1} P_m\right] = \frac{1}{2\pi}\left|\sum_{n=0}^{\infty} \mathrm{e}^{in\phi}\psi_n\right|^2 \tag{2.104}$$

where

$$\phi = \lim_{s\to\infty}\frac{2\pi m}{s+1}\ , \tag{2.105}$$

and ψ_n is the number state coefficient for any Hilbert space state. This convergence in distribution ensures that the moments of the PB Hermitian phase operator converge, as $s\to\infty$, to the moments of the phase probability density.

The phase distribution provides a useful insight into the structure of fluctuations in quantum states. For example, in the number state $|n\rangle$, the mean and variance of the phase distribution are given by

$$\langle\phi\rangle = \phi_0 + \pi\ , \tag{2.106}$$

and

$$V(\phi) = \tfrac{2}{3}\pi\ , \tag{2.107}$$

respectively. These results are characteristic of a state with random phase. In the case of a coherent state $|r\mathrm{e}^{\mathrm{i}\phi}\rangle$ with $r \gg 1$, we find

$$\langle\phi\rangle = \phi\ , \tag{2.108}$$

$$V(\phi) = \frac{1}{4\bar{n}}\ , \tag{2.109}$$

where $\bar{n} = \langle a^\dagger a\rangle = r^2$ is the mean photon number. Not surprisingly a coherent state has well defined phase in the limit of large amplitude.

Exercises

2.1 If $|X_1\rangle$ is an eigenstate for the operator X_1 find $\langle X_1|\psi\rangle$ in the cases (a) $|\psi\rangle = |\alpha\rangle$; (b) $|\psi\rangle = |\alpha, r\rangle$.

2.2 Prove that if $|\psi\rangle$ is a minimum-uncertainty state for the operators X_1 and X_2, then $V(X_1, X_2) = 0$.

2.3 Show that the squeeze operator

$$S(r,\phi) = \exp\left[\frac{r}{2}(\mathrm{e}^{-2\mathrm{i}\phi}a^2 - \mathrm{e}^{2\mathrm{i}\phi}a^{\dagger 2})\right]$$

may be put in the normally ordered form

$$S(r, \phi) = (\cosh r)^{-1/2} \exp\left(-\frac{\Gamma}{2} a^{\dagger 2}\right) \exp[-\ln(\cosh r) a^{\dagger} a] \exp\left(\frac{\Gamma^*}{2} a^2\right)$$

where $\Gamma = e^{2i\phi} \tanh r$.

2.4 Evaluate the mean and variance for the phase operator in the squeezed state $|\alpha, r\rangle$ with α real. Show that for $|r| \gg |\alpha|$ this state has either enhanced or diminished phase uncertainty compared to a coherent state.